Функция релаксации. В общем, ширина релаксационной функции измерена для половины ширины пика потерь и составляет от 4 до 6 декад, но она симметрична. С увеличением температуры ширина β-пика уменьшается. Предполагается, что форма функции релаксации для случая β-релаксации связана с распределением как по энергии активации, так и по предэкспоненциальному множителю, т. е. связана с молекулярным окружением релаксирующих диполей. Обычно сложно получить информацию о преобладающем механизме подвижности, исходя из анализа таких широких релаксационных пиков.

СПИСОК ЛИТЕРАТУРЫ

1. *Белоусов А. М., Пазников Е. А., Орлова Н. А.* Исследование процессов структурирования тетразолсодержащих полимеров различными системами отверждения // Известия высших учебн. завед.: Сер. «Хим. и хим. технология». 2006. Т. 49. № 8. С. 3–9.

2. *Kremer K., Schonhals A.* (Eds.). Broadband dielectric spectroscopy, Springer, Berlin Heidelberg, 2003. 729 с.

REFERENCES

1. *Belousov A. M., Paznikov E. A., Orlova N. A.* Issledovanie protsessov strukturirovanija tetrazolsoderzhashchih polimerov razlichnymi sistemami otverzhdenija // Izv. vyssh. uchebn. zaved.: Ser. "Him. i him. Tehnologija". 2006. Т. 49. № 8. S. 3–9.

2. *Kremer K., Schonhals A.* (Eds.). Broadband dielectric spectroscopy, Springer, Berlin Heidelberg, 2003. 729 с.

D. Rodionov, A. Belyaev, M. Guitou,
A. Spielfiedel, N. Feautrier, P. Barklem

EXTENDED STUDY OF LOW-ENERGY INELASTIC MAGNESIUM-HYDROGEN COLLISIONS

Quantum calculations of cross sections for inelastic processes in Mg + H and $Mg^+ + H$ collisions are improved. It is shown that the largest cross section among the endothermic processes, with a value of approximately 100 $Å^2$, corresponds to the process of ion-pair formation: $Mg(3s4s\,^1S) + H \rightarrow Mg^+ + H^-$. The mechanism of the process is based on nonadiabatic transitions between the $MgH(^2\Sigma^+)$ molecular states, which provide the main mechanism for inelastic processes in Mg + H collisions. On the other hand, nonadiabatic transitions between $MgH(^2\Pi)$ states affect some cross sections rather significantly. For example, transitions between the $MgH(^2\Pi)$ states increase the cross section for the excitation process $Mg(3s3p\,^1P) + H \rightarrow Mg(3s3d\,^1D) + H$ by almost an order of magnitude as compared to the cross section obtained within the $MgH(^2\Sigma^+)$ symmetry.

Keywords: atomic collisions, nonadiabatic transitions, inelastic cross sections.

Д. С. Родионов, А. К. Беляев, М. Гиту,

А. Спилфидель, Н. Фотриер, П. С. Барклем

РАСШИРЕННОЕ ИЗУЧЕНИЕ НЕУПРУГИХ НИЗКОЭНЕРГЕТИЧЕСКИХ MG + H СТОЛКНОВЕНИЙ

Улучшены квантовые расчёты сечений неупругих процессов Mg + H и Mg$^+$ + H$^-$. Показано, что наибольшее сечение среди эндотермических процессов со значением примерно 100 Å^2 соответствует процессу формирования ионной пары: Mg(3s4s ^{1}S) + H → Mg$^+$ + H$^-$. Доминирующим механизмом неупругих процессов, рассмотренных в данной работе, являются переходы между MgH($^2\Sigma^+$) молекулярными состояниями. С другой стороны, неадиабатические переходы между MgH($^2\Pi$) молекулярными состояниями могут значительно повлиять на некоторые сечения. Например, переходы между MgH($^2\Pi$) состояниями увеличивают сечение процесса возбуждения Mg(3s3p ^{1}P) + H → Mg(3s3d ^{1}D) + H почти на порядок, по сравнению с сечением, полученным с учётом только MgH($^2\Sigma^+$) симметрии.

Ключевые слова: атомные столкновения, неадиабатические переходы, неупругие сечения.

1. Introduction

The measurement of abundances of chemical elements in stellar atmospheres, as interpreted from stellar spectra, is of fundamental importance in modern astrophysics, see, e.g., [16, 2, 20]. Inelastic processes in collisions of different atoms with hydrogen atoms are important for the non-local thermodynamic equilibrium modeling of stellar spectra which is the main tool for relative and absolute chemical abundances, see, e.g., [2, 3]. Magnesium is an element of significant astrophysical importance, see [1, 19] and references therein. Thus, the need for investigation of inelastic collisions of hydrogen atoms with magnesium atoms is well justified.

In the earlier works, Ref. [14, 9] quantum dynamical calculations have been performed for three MgH($^2\Sigma^+$) plus two MgH($^2\Pi$) molecular states, as well as for the eight lowest-lying MgH($^2\Sigma^+$) states, respectively, based on accurate *ab initio* quantum chemical data [15]. In Ref. [12] it was shown that among the low-lying states the transitions between $^2\Sigma^+$ molecular states dominate over transitions involving states of other symmetries. For this reason, the inelastic cross sections were calculated in Ref. [9] by taking into account only the transitions between the eight lowest-lying MgH($^2\Sigma^+$) states. In the present paper, we extend the earlier work in Ref. [9] through a calculation including nine $^2\Sigma^+$ states up to and including the ionic channel, and the five lowest $^2\Pi$ states based on improved *ab initio* quantum-chemical data.

2. MgH interaction potentials, nonadiabatic couplings and cross sections
2.1. Ab initio quantum-chemical calculations

The adiabatic potentials and nonadiabatic couplings were calculated using large active spaces and basis sets since avoided crossings occur due to the Mg$^+$ + H$^-$ ionic configuration [15]. All $^2\Sigma^+$, $^2\Pi$, $^2\Delta$, $^4\Sigma^+$ and $^4\Pi$ electronic molecular states arising from Mg + H for energies up to about 6 eV above the lowest atomic asymptote Mg(^{1}S) + H(^{2}S$_g$) were calculated at the MRCI

level, as well as the couplings between these states. The details are described in Refs. [14, 15]. These new potentials (and couplings) are improved thanks to of an extension of the basis set, comparing to ones used in Refs. [14, 15]. The presently used basis set is larger and will be published elsewhere.

Table 1

The MgH molecular channels, the corresponding asymptotic atomic states and the calculated and experimental (NIST [20] weighted average values) asymptotic energies with respect to the ground state. Some calculated asymptotic values were adjusted to fit the experimental data

j	Molecular states	Atomic asymptotic states	Asymptotic energies (eV)	
			Calculation	Experiment
1	$1\,^2\Sigma^+$	$Mg(3s^2\,^1S) + H$	0.0	0.0
2	$2\,^2\Sigma^+$	$Mg(3s3p\,^3P) + H$	2.7142	2.7142
3	$3\,^2\Sigma^+$	$Mg(3s3p\,^1P) + H$	4.3894	4.3458
4	$4\,^2\Sigma^+$	$Mg(3s4s\,^3S) + H$	5.1342	5.1078
5	$5\,^2\Sigma^+$	$Mg(3s4s\,^1S) + H$	5.4237	5.3937
6	$6\,^2\Sigma^+$	$Mg(3s3d\,^1D) + H$	5.7532	5.7532
7	$7\,^2\Sigma^+$	$Mg(3s4p\,^3P) + H$	5.9321	5.9321
8	$8\,^2\Sigma^+$	$Mg(3s3d\,^3D) + H$	5.9460	5.9459
9	$9\,^2\Sigma^+$	$Mg^+(3s\,^2S) + H^-$	6.8916	6.8916
10	$1\,^2\Pi$	$Mg(3s3p\,^3P) + H$	2.7142	2.7142
11	$2\,^2\Pi$	$Mg(3s3p\,^1P) + H$	4.3894	4.3458
12	$3\,^2\Pi$	$Mg(3s3d\,^1D) + H$	5.7532	5.7532
13	$4\,^2\Pi$	$Mg(3s4p\,^3P) + H$	5.9321	5.9321
14	$5\,^2\Pi$	$Mg(3s3d\,^3D) + H$	5.9460	5.9459

The nine lowest MgH($^2\Sigma^+$) and the five lowest MgH($^2\Pi$) molecular states treated in the present work are collected in table 1, including their asymptotic atomic limits. The corresponding potential energy curves (PECs) are represented in figs. 1 as a function of the internuclear distance.
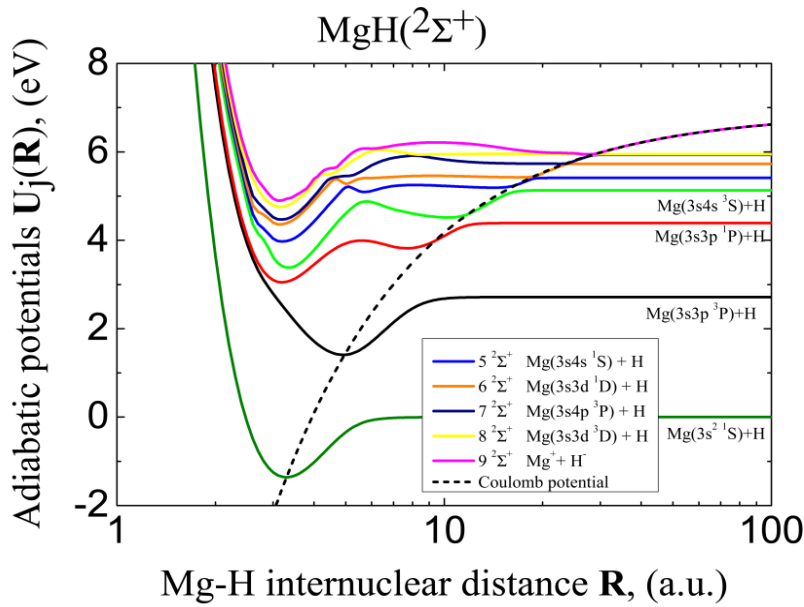
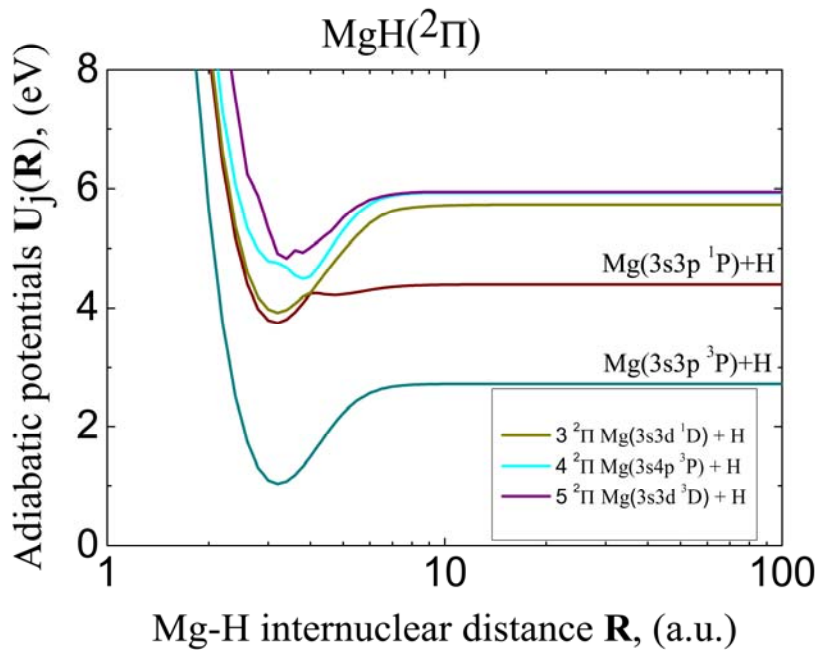*Fig. 1.* Potential energy curves for the lowest nine MgH($^2\Sigma^+$) states

Fig. 2. Potential energy curves for the lowest five MgH($^2\Sigma^+$) states

A series of avoided crossings for the $^2\Sigma^+$ states is clearly seen. The background of these avoided crossings is an interaction of covalent states with the $Mg^+ + H^-$ ionic state. For the high-lying molecular states the avoided crossings occur at large distances with small adiabatic splittings. These avoided crossings provide the main mechanism for inelastic processes in low-energy Mg + H collisions, that is, for the processes of excitation, de-excitation, ion-pair production, and mutual neutralization. The nonadiabatic couplings needed for performing quantum dynamical calculations are depicted in figs. 3 and 4. They clearly confirm the presence of the nonadiabatic regions, where nonadiabatic transitions take place.
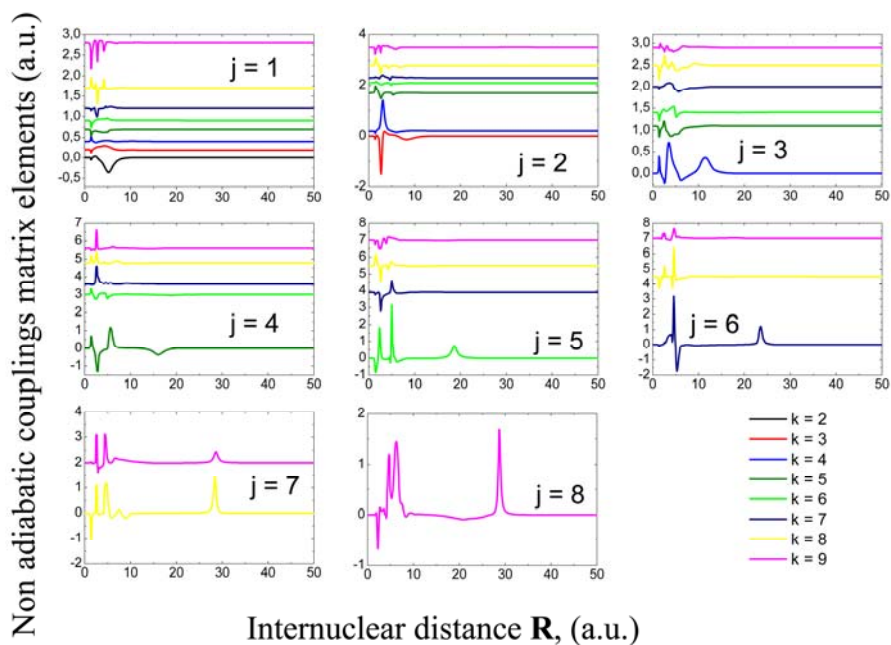
Fig. 3. Nonadiabatic radial coupling matrix elements $\left\langle j \left| \dfrac{d}{dR} \right| k \right\rangle$ plus offsets,

between the nine MgH($^2\Sigma^+$) states used in the present study. The molecular state label j is indicated in each panel. The keys for the labels k are given in the right panel and are common to all panels. Offsets are used for better representation of the radial couplings
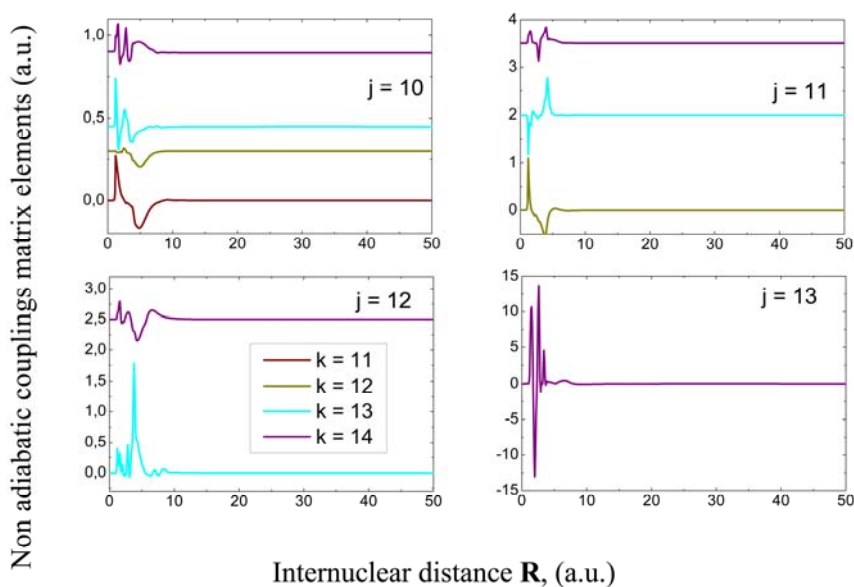

Fig. 4. Nonadiabatic radial coupling matrix elements $\left\langle j \left| \dfrac{d}{dR} \right| k \right\rangle$ plus offsets,

between the five MgH($^2\Pi$) states used in the present study. The molecular state label j is indicated in each panel. The keys for the labels k are given in the right panel and are common to all panels. Offsets are used for better representation of the radial couplings

It is worth emphasizing that the five lowest MgH($^2\Sigma^+$) molecular states have practically the same adiabatic potentials and nonadiabatic couplings as in the previous calculations [14, 9, 15]. The improvement mainly concerns the higher-lying states, starting from $j = 6$. Thus, inelastic cross sections obtained with the more accurate quantum-chemical data presented here may be expected to deviate more substantially for processes involving high-lying states.

2.2. Nonadiabatic nuclear dynamics

The nonadiabatic nuclear dynamical calculations are carried out within the standard adiabatic Born-Oppenheimer approach by means of the multi-electron reprojection method [6] (see also references therein) to account for the so-called electron translation problem. The method takes into account non-vanishing asymptotic nonadiabatic matrix elements, provides the correct incoming and outgoing asymptotic total wave functions, and removes nonadiabatic transitions between atomic-state channels in the asymptotic region. First, the nuclear dynamics was performed for the three low-lying $^2\Sigma^+$ and the first two $^2\Pi$ states [14]. It was concluded that the main mechanism for nonadiabatic transitions between molecular states at low energies is due to the radial couplings associated with the avoided ionic crossings in the $^2\Sigma^+$ symmetry. The same mechanism, though in the $^1\Sigma^+$ symmetry, was found to be dominant in calculations for Li + H and Na + H low-energy collisions [10, 11, 12, 13, 7, 8]. Based on this conclusion, the nonadiabatic dynamics is then studied for the eight lowest molecular states in the $^2\Sigma^+$ symmetry including the ionic channel [5], as the astrophysical applications [19, 4, 17, 18] show the importance of ion-pair production processes.

In the present study, the inelastic cross sections for Mg + H and Mg$^+$ + H$^-$ collisions are calculated for all transitions between the nine lowest $^2\Sigma^+$ symmetry states, as well as for all transitions between the five lowest $^2\Pi$ symmetry states, based on the improved quantum-chemical data. The cross sections calculated within the $^2\Sigma^+$ symmetry for the endothermic processes are presented in fig. 5 for each particular initial channel. The collision energy E is the kinetic energy in a given initial channel. The comparison of the present cross sections with those obtained in Ref. [9] shows that the calculations are stable, though some cross sections deviate due to the new and more accurate quantum-chemical data. It is seen that the ion-pair formation process, Mg(3s4s ^{1}S) + H → Mg$^+$ + H$^-$, has the largest cross section, of approximately 107 Å^2, among the endothermic processes.

The previously calculated cross section for the same process had a value of 100 Å^2 [9], that is, the deviation is within a few percent. This is within the expected accuracy of 20 % [5].
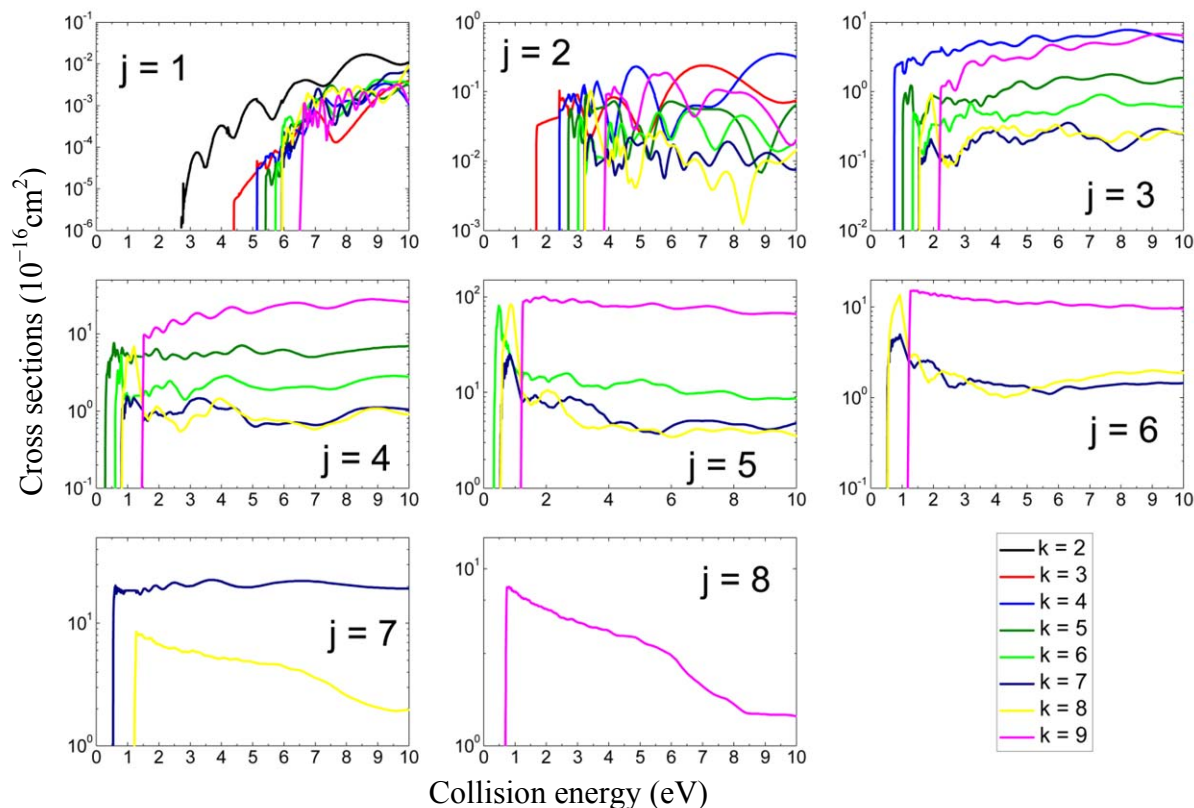
Fig. 5. The inelastic cross sections $\sigma_{jk}(E)$ for transitions $j \rightarrow k$ ($k > j$) in low-energy Mg + H collisions. The label j of the initial state from which transitions occur is indicated in each panel. The key for the final states k is given in the bottom right panel

Nonadiabatic transitions between MgH($^2\Pi$) states may affect the excitation (but not ion-pair formation nor mutual neutralization) cross sections due to transitions between highly excited states of magnesium atoms colliding with hydrogen atoms. The inelastic cross sections calculated within the $^2\Pi$ symmetry are shown in Fig. [6]. The labels for the processes within the MgH($^2\Pi$) are presented in table 1. One should keep in mind that not all atomic channels collected in table 1 can produce MgH($^2\Pi$) molecular channels. Thus, the inclusion of the additional channels of the MgH($^2\Pi$) molecular symmetry increases inelastic cross sections for those transitions that can occur within both the MgH($^2\Pi$) and the MgH($^2\Sigma^+$) symmetries.

For example, in the case of the excitation process Mg(3s3p ^{1}P)+H $\rightarrow$ Mg(3s3d ^{1}D) + H, accounting for transitions between the MgH($^2\Pi$) states increases the cross section by almost an order of magnitude as compared with the cross section obtained within the MgH($^2\Sigma^+$) states.

The importance of $^2\Pi$ channels should be confirmed by taking into account the rotational couplings that mix Σ and Π states. This work is in progress.
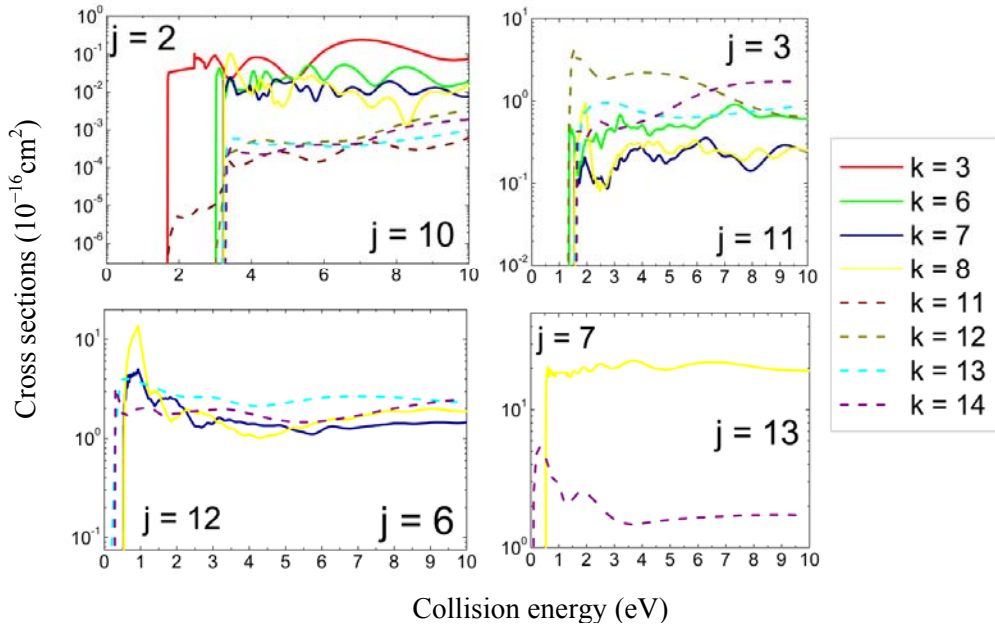
Fig. 6. The inelastic cross sections $\sigma_{jk}(E)$ for transitions $j \to k$ ($k > j$)
in low-energy Mg + H collisions calculated within the $^2\Sigma^+$ symmetry (solid lines)
and within the $^2\Pi$ symmetry (dashed lines). Note that only the transitions corresponding to the same initial and the same final atomic states of Mg but occurring in different molecular symmetries ($^2\Sigma^+$ and $^2\Pi$) are presented in the figure. For example, the transitions $j = 3 \to k = 6$ and $j = 11 \to k = 12$ correspond to the excitation Mg(3s3p ^{1}P $\to$ 3s3d ^{1}D) + H in the $^2\Sigma^+$ and $^2\Pi$ symmetries, respectively

The physics for the inelastic processes in the treated collisions was carefully studied in Ref. [9] and several mechanisms were found. The present calculations confirm the previous conclusions. It is shown that some of the mechanisms are determined by interactions between adjacent molecular states due to interactions between ionic and covalent configurations. However, mechanisms at short distances, not restricted to adjacent states, are found to be important for some processes. These mechanisms explain the relatively large cross sections for excitation of highly excited states.

3. Concluding remarks

In the present study, the cross sections for the inelastic processes in Mg + H and Mg$^+$ + H$^-$ collisions are calculated based on improved quantum-chemical data and on estimates of accounting for nonadiabatic transitions not only in the MgH($^2\Sigma^+$) symmetry, but also in the MgH($^2\Pi$) symmetry. It is shown that the process of ion pair formation: Mg(3s4s ^{1}S) + H $\to$ Mg$^+$ + H$^-$ has the largest cross section, approximately 100 Å^2, among the endothermic processes. This process occurs due to the nonadiabatic transitions between the $^2\Sigma^+$ states. On the other hand, nonadiabatic transitions between MgH($^2\Pi$) states significantly affect some excitation cross sections due to transitions between highly excited states of magnesium atoms colliding with hydrogen. As an example, accounting for transitions between the MgH($^2\Pi$) states increases the cross section for the excitation process Mg(3s3p ^{1}P) + H $\to$ Mg(3s3d ^{1}D) + H by almost an order of magnitude as compared with the cross section obtained within the MgH($^2\Sigma^+$) symmetry.

70

4. Acknowledgements

REFERENCES

1. *Arnone E., Ryan S.G., Argast D., Norris J.E. and Beers T.C.* Mg abundances in metal-poor halo stars as a tracer of early Galactic mixing // Astronomy & Astrophysics. 2005. V.430. P. 507–522.

2. *Asplund M.* New light on stellar abundance analyses: Departures from LTE and Homogeneity // Annual Review of Astronomy and Astrophysics. 2005. V. 43. P. 481–530.

3. *Barklem P. S.* Hydrogen Atom Collision Processes in Cool Stellar Atmospheres: Effects on Spectral Line Strengths and Measured Chemical Abundances in Old Stars // Journal of Physics: Conference Series. 2012. V. 397. Art. num. 012049.

4. *Barklem P.S., Belyaev A.K. and Asplund M.* Inelastic H + Li and H- + Li+ collisions and non-LTE Li I line formation in stellar atmospheres // Astronomy & Astrophysics. 2003. V.409. P. L1–L4.

5. *Barklem P. S., Belyaev A. K., Spielfiedel A., Guitou M. and Feautrier N.* Inelastic Mg + H collision data for non-LTE applications in stellar atmospheres // Astronomy & Astrophysics. 2012. V. 541. Art. num. A80.

6. *Belyaev A. K.* Revised Born-Oppenheimer approach and a reproection method for inelastic collisions // Physical Review A. 2010. V.82. Art. num. 060701(R).

7. *Belyaev A. K. and Barklem P. S.* Cross sections for low-energy inelastic H + Li collisions // Physical Review A. 2003. V.68. Art. num. 062703.

8. *Belyaev A.K., Barklem P.S., Dickinson A.S. and Gadéa F.X.* Cross sections for low-energy inelastic H + Na collisions // Physical Review A. 2010. V.81. Art. num. 032706.

9. *Belyaev A.K., Barklem P.S., Spielfiedel A., Guitou M., Feautrier N., Rodionov D.S. and Vlasov D.V.* Cross sections for low-energy inelastic Mg + H and Mg+ + H− collisions // Physical Review A. 2012. V.85. Art. num. 032704.

10. *Belyaev A.K., Grosser J., Hahne J. and Menzel T.* Ab initio cross sections for low-energy inelastic H + Na collisions // Physical Review A. 1999. V.60. Pp.2151–2158.

11. *Croft H., Dickinson A.S. and Gadéa F.X.* Rate coefficients for the Li+/H− and Li−/H+ mutual neutralization reactions // Monthly Notices of the Royal Astronomical Society. 1999. V.304. Issue 2. P. 327–329.

12. *Croft H., Dickinson A.S. and Gadéa F.X.* A theoretical study of mutual neutralization in Li + H collisions // Journal of Physics B: Atomic, Molecular and Optical Physics. 1999. V.32. N.1. Pp. 81–94.

13. *Dickinson A.S., Poteau R. and Gadéa F.X.* An ab initio study of mutual neutralization in Na+ + H- collisions // Journal of Physics B: Atomic, Molecular and Optical Physics. 1999. V. 32. N. 23. P. 5451–5462.

14. *Guitou M., Belyaev A.K., Barklem P.S., Spielfiedel A. and Feautrier N.* Inelastic Mg + H collision processes at low energies // Journal of Physics B: Atomic, Molecular and Optical Physics. 2011. V.44. Art. num. 035202.

15. *Guitou M., Spielfiedel A. and Feautrier N.* Accurate potential energy functions and non-adiabatic couplings in the Mg + H system // Chemical Physics Letters. 2010. V. 488. Issues. 4–6. P. 145–152.

16. *Lambert D. L.* Quantitative stellar spectroscopy with large optical telescopes // Physica Scripta. 1993. V. T47. P. 186–198.

17. *Lind K., Asplund M. and Barklem P. S.* Departures from LTE for neutral Li in late-type stars // Astronomy & Astrophysics. 2009. V. 503 P. 541–544.

18. *Lind K., Asplund M., Barklem P.S. and Belyaev A.K.* Non-LTE calculations for neutral Na in late-type stars using improved atomic data // Astronomy & Astrophysics. 2011. V. 528. Art. num. A103.

19. *Mashonkina L.* Astrophysical tests of atomic data important for the stellar Mg abundance determinations // Astronomy & Astrophysics. 2013. V. 550. art. num. A28.

20. *Ralchenko Y., Kramida A. E. and Reader J.* (NIST ASD Team), NIST Atomic Spectra Database (version 3.1.4), Gaithersburg, MD,USA: National Institute of Standards and Technology. 2008. [http: //physics.nist.gov/asd3].